Doubly resonant LO-phonon Raman scattering observed with GaAs-$Al_xGa_{1-x}As$ quantum wells

D. A. Kleinman, R. C. Miller, and A. C. Gossard
AT&T Bell Laboratories, Murray Hill, New Jersey 07974-2070
(Received 31 March 1986; revised manuscript received 27 August 1986)

Very sharp line emission has been seen in the $n=1$ heavy-hole exciton E_{1h} luminescence of certain GaAs-$Ga_{1-x}Al_xAs$ quantum-well structures under optical excitation at $E_{1h}+n\hbar\omega_{LO}$ ($n=1,2,3,4$) where $\hbar\omega_{LO}=36.7$ meV is the LO-phonon energy of GaAs. The samples showing this effect all have a resonance between $E_{1h}+\hbar\omega_{LO}$ and some higher excitonic transition, in most cases the nominally forbidden transition involving the $n=1$ electron and $n=3$ heavy hole, E_{13h}. The effect, which we call doubly resonant Raman scattering (DRRS), has been seen for excitation with E_{13h} and E_{2h} in square-well structures and resonant with E_{21h} in one half-parabolic-well sample. The DRRS line has nearly three times the circular polarization of the broad ordinary luminescence and a large linear polarization (optical alignment) not usually seen in luminescence from quantum wells. The polarization properties of DRRS at 6 K for one sample have been completely determined, as well as the magnitude of the scattering relative to the ordinary luminescence. A theoretical discussion is given for the first-order DRRS characterizing the principal mechanisms, the strength, the LO-phonon involved, the effects of symmetry, and polarization relaxation. It is concluded that the Fröhlich interaction can account for the strength but there could also be significant impurity-assisted Fröhlich scattering, the deformation potential interaction is negligible, and the polarization relaxation suggests as much as 55% impurity-assisted scattering.

I. INTRODUCTION

The observation of Raman scattering resonant with excitons in GaAs-$Al_xGa_{1-x}As$ quantum-well (square-well) structures has been reported previously.[1–4] Enhanced Raman scattering was observed when either the incident photon energy or the scattered photon energy was resonant with a quantum-well exciton transition in which the electron and hole possessed the same confinement quantum number n. This paper describes the first resonant Raman scattering (RRS) with GaAs quantum wells where the incident and scattered photon energies are both resonant with an exciton transition. Furthermore, in the sample studied in detail (principal sample) the incident resonance involves different confinement states for the electron and hole. This type of resonant Raman scattering will be termed "doubly resonant Raman scattering" (DRRS). As many as four sharp peaks separated by the longitudinal optic (LO) phonon energy $\hbar\omega_{LO}$ have been seen in excitation spectra of samples which exhibit DRRS. These peaks seen in excitation, and the relatively strong sharp peak (FWHM$\sim$0.4 meV) seen in emission under DRRS, all exhibit substantial optical alignment as well as strong circular polarization.

Phonon-assisted transitions seen in excitation have been observed at 6 K with many GaAs quantum-well structures including those with many wells, single wells, and half-parabolic wells. One sample was grown by metalorganic vapor deposition while the remainder were grown by molecular-beam epitaxy (MBE). The structures all exhibited two exciton transitions, one of which was in emission, separated in energy by $\hbar\omega_{LO}$, and their photoluminescence efficiencies were generally down from the brightest samples by one or more orders of magnitude. The principal sample containing 50 GaAs quantum wells with $L_z=140$ Å separated by 193 Å $x=0.33$ alloy barriers was grown by MBE on a (100) Cr-doped semi-insulating GaAs substrate.

II. EXPERIMENTAL PROCEDURE AND RESULTS

The photoluminescence (PL) and excitation spectra obtained in the backscattering direction at 24° from normal to the layer for the principal sample at 6 K are shown in Fig. 1. All data presented in the figures in this manuscript were obtained with a detection resolution of FWHM=0.20 meV, which results in a measured excitation dye laser linewidth of FWHM$\approx$0.35 meV. The laser was a Kr-pumped tunable cw dye laser. For the PL spectrum, excitation was with 6.2 W/cm^2 at 1.568 eV. This excitation photon energy is resonant with the $\Delta n=2$ exciton transition between the $n=1$ electron and the $n=3$ heavy hole, denoted E_{13h}.[5,6] The unique feature in the PL spectrum is the sharp peak at 1.533 eV. Other data (not shown) taken at higher detection resolution (0.15 meV) led to measured widths FWHM$\sim$0.33 and 0.38 meV for the exciting laser beam and sharp PL peak, respectively.

The excitation spectrum given in Fig. 1 was obtained by scanning the incident photon energy with detection of the PL set on the sharp DRRS peak. Calculated energies of some of the usual exciton quantum-well transitions are indicated by short vertical arrows. The $\Delta n=0$ transitions are labeled by E_{ij} where $i=n$ and j gives the hole character h or l, for heavy and light holes, respectively. These exciton transitions, which show up more clearly with detection shifted to the broad PL peak (1.529 eV), were

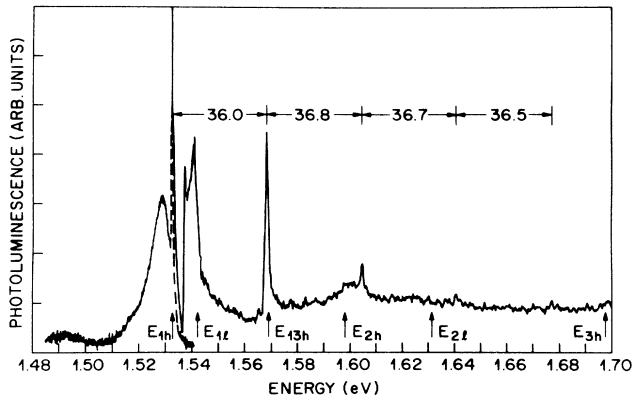

FIG. 1. Photoluminescence (dashed and solid curve on the left-hand side), and excitation (solid curve on the right-hand side), spectra at 6 K for a GaAs quantum-well sample with 50 periods of 140 Å wells and 193 Å $x=0.33$ alloy barriers. For the photoluminescence spectrum, the sample was excited at $E_{13h}=1.5680$ eV. The excitation spectrum was obtained by scanning the incident photon energy E_p with the detector set at 1.5326 eV. The detector sensitivity was decreased by 10 for $E_p<1.538$ eV. The measured intervals equal to $\hbar\omega_{LO}$ between the sharp peaks in the excitation spectrum are given in meV and are believed accurate to ±0.3 meV. Calculated exciton transition energies are indicated by short vertical arrows below the excitation spectrum.

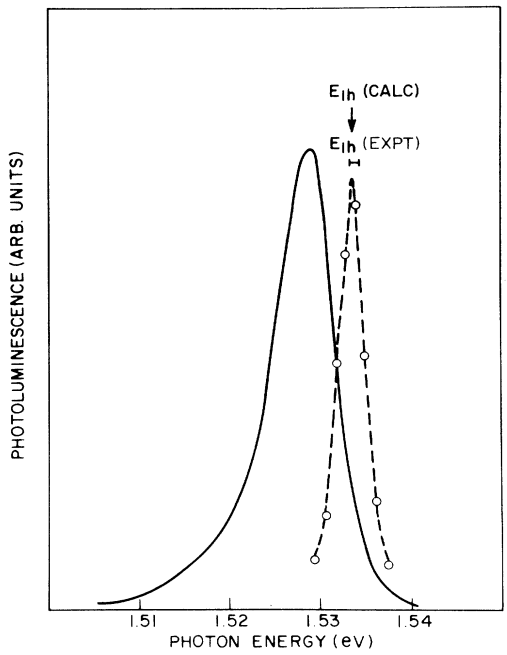

FIG. 2. Photoluminescence intensity, solid curve, at 6 K in the absence of DRRS and the amplitude of the DRRS signal, dashed curve, as the excitation photon energy is scanned through E_{13h}. The calculated and measured photon energies of the E_{1h} exciton peak are also shown. The energy of the DRRS peak and its FWHM=4.2 meV are in good agreement with that observed for E_{1h} as seen in excitation (not shown).

used to estimate the quantum-well width, $L_z=140$ Å. The transition energies shown in Fig. 1 were calculated as described in Ref. 7 using a nonparabolic conduction band for GaAs and valence-band offset equal to 40% of the band-gap discontinuity between the GaAs and $Al_xGa_{1-x}As$ layers.

The four sharp peaks in the excitation spectra are reproducible and are attributed to phonon-assisted transitions. The separations between these peaks given in the figure in meV are estimated to be accurate to ±0.3 meV and are in good agreement with $\hbar\omega_{LO}$ for bulk GaAs,[8,9] namely, 36.7 meV. When the detection energy is changed, the phonon-associated peaks, and not the exciton transitions, move along with it preserving their $\hbar\omega_{LO}$-like intervals. This has been observed for shifts to higher and lower energies from that shown in Fig. 1 by as much as 4 meV. As shown in Fig. 2, a plot of the amplitude of the sharp single-phonon DRRS peak versus energy shows a width FWHM≈4.2 meV which is in good agreement with that seen for E_{1h} in excitation, namely 4 meV±1 meV. Also the maximum amplitude of the sharp PL peak occurs at the observed E_{1h}, 1.5340 eV±0.5 meV. No luminescence at E_{13h} was observed when exciting at $E_{13h}+n\hbar\omega_{LO}$, $n=1,2,3$.

Limited data show that these phonon-associated peaks are not very sensitive to either the excitation intensity I_p or the sample temperature T. The variation of the amplitudes of the sharp and broad PL peaks expressed as I_p^{α} is approximated by $\alpha\sim0.93$ and 1.4, respectfully. When T is increased from 6 to 80 K, the sharp DRRS peak in the PL decreases by a factor ≈4 while the main PL peak decreases by a factor ≈50.

Data have also been obtained using both circular and linear polarization techniques. For resonant excitation at E_{13h} as in Fig. 1 the observed circular polarization at the DRRS peak was the same sign (+) as that of the excitation and very large (77%), nearly 3 times that for the broad PL peak (27%). Signal-to-noise problems made similar measurements difficult to make at the other phonon-associated peaks in the excitation spectrum, but an increase in positive polarization could be detected for excitation at the phonon peak on the high-energy side of E_{2h}.

Of even more interest are the measurements of linear polarization, which is not usually observed in the PL of GaAs quantum-well samples. Following Menéndez and Cardona,[10] we define the directions $x[1,0,0]$, $y[0,1,0]$, $x'[1,1,0]$, and $y'[1,\bar{1},0]$ in the plane of the quantum well and $z[0,0,1]$ normal to the well. Figure 3(a) shows, for example, the PL spectra at 6 K with resonant excitation at E_{13h} for the excitation-detection configurations $z(y',y')\bar{z}$ and $z(y',x')\bar{z}$. These data give a linear polarization of +53% at the DRRS peak and at most −3% elsewhere, which is believed to be instrumental in origin. A summary of the DRRS polarization data (integrated intensities) on the principal sample is given in Table I. The different configurations were obtained on the same sample, incident beam, and detection system by changing only the input and output polarizers. The uncertainties indicated in Table I are a measure of the scatter of the measurements from run to run. The V notation for polarization

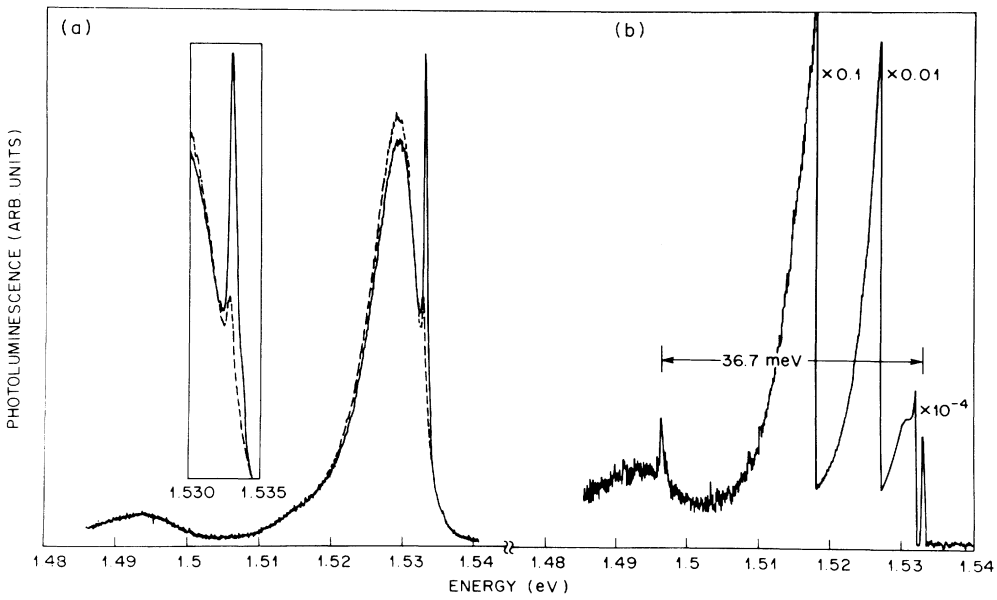

FIG. 3. Photoluminescence spectra at 6 K for the principal sample. (a) Spectra are shown for resonant excitation at $E_{13h}=1.5680$ eV for the excitation and detection linear polarizers parallel, $z(y',y')\bar{z}$, (solid line), and crossed, $z(x',y')\bar{z}$, dashed line. The linear polarization of the sharp peak in this case is $+0.53$ with the parallel configuration giving the larger signal. The background polarization of -3% is believed to be instrumental. (b) The photoluminescence spectrum is shown for resonant excitation at 1.533 eV. A resonant Raman peak is observed $\hbar\omega_{\rm LO}$ below the excitation photon energy.

configurations to be used later is defined in Eq. (22). The three higher-energy phonon-associated peaks show linear polarizations $\sim 25\%$.

Most of the wafers which have exhibited DRRS were structures for which E_{13h}-$E_{1h}\approx\hbar\omega_{\rm LO}$. One interesting exception was a wafer which contained 20 half-parabolic wells grown by MBE as described in Ref. 11. An analysis of the energies of the exciton transitions seen in the excitation spectrum for this structure shows that the energy intervals between successive excitons from $n=1$ to 4 in the conduction band are very nearly constant as expected and have an average value of 36.7 meV, i.e., equal to $\hbar\omega_{\rm LO}$. For this case with detection set at E_{1h} a sharp phonon peak is seen in the excitation spectrum at $E_{21h}=E_{1h}+\hbar\omega_{\rm LO}$, and a weaker sharp peak at $E_{1h}+2\hbar\omega_{\rm LO}$ which is therefore coincident energywise with the expected position of the E_{31h} exciton transition. Also several wafers with $L_z\approx 190$ Å exhibited DRRS with emission at E_{1l} and excitation at E_{2h}.

We have estimated the PL quantum efficiency of the principle sample by comparing the integrated PL intensity with that for one of the brightest samples we have ever studied with the pump photon energy in each case at $E_p=E_{2h}$. The principle sample ($L_z=140$ Å) was down from the bright sample ($L_z=145$ Å) by a factor ≈ 124. On the reasonable assumption that the bright sample has near unity quantum efficiency, we estimate $\eta\sim 8.1\times 10^{-3}$ for the quantum efficiency of the principle sample.

The phonon-assisted transitions described above have resulted from excitations at energies $\geq\hbar\omega_{\rm LO}$ above the exciton energy gap of the quantum-well sample. It has also been observed that if the principal sample is excited resonantly with the E_{1h} exciton transition a satellite peak appears in the emission spectrum shifted by $\hbar\omega_{\rm LO}$ to lower energies. This RRS is shown in Fig. 3(b); in this case the amplitude of the satellite peak is about 0.5% of the main broad PL peak. The LO-phonon-shifted peak moves with the excitation line and is observed with the principal sample as long as the excitation is within the E_{1h} exciton peak.

TABLE I. Measured integrated intensity for principal sample of single-LO-phonon DRRS for various excitation-detection polarization configurations. The configurations are defined following Eq. (25) and the **V** notation in Eq. (27). The measured values are normalized to make $z(+,+)\bar{z}+z(+,-)\bar{z}=1$.

Configuration	**V** notation	Measured
$z(+,+)\bar{z}$	(1,0,0,0)	0.885 ∓ 0.005
$z(+,-)\bar{z}$	(0,1,0,0)	0.115 ± 0.005
$z(x,x)\bar{z}$	(1,1,1,1)/2	0.79 ± 0.02
$z(y,x)\bar{z}$	$i(1,1,-1,-1)/2$	0.23 ± 0.04
$z(x',x')\bar{z}$	$(1,i,-i,1)/2$	0.75 ± 0.04
$z(y',y')\bar{z}$	$(1,-i,i,1)/2$	0.82 ± 0.02
$z(y',x')\bar{z}$	$(-i,1,1,i)/2$	0.27 ± 0.04

III. THEORETICAL DISCUSSION

The following discussion is mainly concerned with the principal sample and the data of Table I. The one-LO-phonon DRRS shown in Fig. 1 is mainly due to the process[1,12,13]

$$R_i \xrightarrow{\text{A·p}} (X_{13h}) \xrightarrow{F} (X_{1h}+L) \xrightarrow{\text{A·p}} R_s+L\ , \tag{1}$$

where R, X, and L denote photons, excitons, and LO phonons, respectively, $\mathbf{A}\cdot\mathbf{p}$ is the photon-exciton interaction, and F is the electrostatic polar (Fröhlich) interaction. Anisotropy[14] of the phonons will be neglected and the phonons will be regarded as those of bulk GaAs. All of the particles in Eq. (1) have zero momentum in the (x,y) plane of the quantum well, but L may have arbitrary momentum in the z direction. The excitons X are in the $1s$ ground state for the relative (x,y) electron-hole motion but may have various configurations (noted where necessary) in regard to the single-well confinement states for the electron and hole (n_e,n_h), and the corresponding spin labels (c,v), where for electrons $c=\pm\frac{1}{2}$, $v=\pm\frac{3}{2}$ for heavy holes, and $v=\pm\frac{1}{2}$ for light holes.[15,16] The photons R are specified by frequency ω and polarization unit vector $\hat{\boldsymbol{\mu}}$, and where appropriate, an exciton created by photon R^{μ} can be indicated by X^{μ} which uniquely specifies (c,v) if heavy (h) or light (l) is also indicated. The intermediate states in parentheses in Eq. (1) in general need not be resonant with the initial or final state, but the case of resonance is indicated by the solid arrow. Our model neglects confinement[2] and zone folding[9] of the phonons and umklapp[4] scattering of the excitons, which is consistent with our observing the same effect in single-well and many-well samples.

There exists a similar intrinsic process through the deformation potential interaction (D) (Refs. 10 and 12)

$$R_i \xrightarrow{\mathbf{A}\cdot\mathbf{p}} (X_{13h}) - - \xrightarrow{D} (X_{1l}+L) - - \xrightarrow{\mathbf{A}\cdot\mathbf{p}} R_s+L \tag{2}$$

which involves a nonresonant scattering to the light-hole exciton X_{1l}. In Eq. (1) both intermediate states are resonant (DRRS), in Eq. (2) only one intermediate state is resonant (RRS), so we would expect the former to be the dominant process.

There is also an extrinsic DRRS process closely related to Eq. (1),[10] the FI process,

$$R_i \xrightarrow{\mathbf{A}\cdot\mathbf{p}} (X_{13h}) - - \xrightarrow{I} (X'_{13h}) - - \xrightarrow{F} (X_{1h}+L') \xrightarrow{\mathbf{A}\cdot\mathbf{p}} R_s+L' , \tag{3a}$$

$$R_i \xrightarrow{} (X_{13h}) - - \xrightarrow{F} (X'_{1h}+L') - - \xrightarrow{I} (X_{1h}+L') \xrightarrow{} R_s+L' , \tag{3b}$$

which involves a static scattering interaction I due to impurities and excitons X' and phonons L' having nonzero momentum in the (x,y) plane. The middle intermediate state is off resonant by the amount of the kinetic energy of the scattered exciton X'. The processes of Eqs. (1) and (2) might involve the same initial and final states (interference) (unless forbidden by the symmetry of L), whereas the process of Eq. (3) necessarily involves a different phonon (no interference) from that in Eqs. (1) and (2).[10] For the three-dimensional (3D) case, where phonon momentum is fixed by momentum conservation, Menéndez and Cardona[10] have used the interference between the F and D mechanisms in several polarizations to explain the observed line shape of the single-LO-phonon RRS in GaAs and determine (for a particular sample) the contribution of the FI mechanism. The FI process has the same polarization properties as the F process.

The matrix elements of the Fröhlich interaction can be written approximately[13]

$$\langle X',L \mid H_F \mid X'' \rangle = -iC_F V_N^{-1/2} \delta_{K'+Q,K''} \delta_{c'c''} \delta_{v'v''} \mid \mathbf{Q}+q\hat{\mathbf{z}} \mid^{-1} \times [\langle n'_e \mid e^{-iqz} \mid n''_e \rangle \delta_{n'_h n''_h} \langle \lambda' \mid e^{-i\mathbf{Q}\cdot\mathbf{r}m_{ht}/M} \mid \lambda \rangle - \langle n''_h \mid e^{-iqz} \mid n'_h \rangle \delta_{n'_e n''_e} \mid \langle \lambda' \mid e^{i\mathbf{Q}\cdot\mathbf{r}m_e/M} \mid \lambda \rangle] \tag{4}$$

where $\mathbf{K},\mathbf{Q}$ are exciton and phonon wave vectors in the (x,y) plane, q the phonon wave vector along $\hat{\mathbf{z}}$, m_e and m_{ht} are the electron and hole transverse effective masses (in units of the free electron mass m_0) for motion in the (x,y) plane and $M=m_e+m_{ht}$, $\mathbf{r}=\mathbf{r}_e-\mathbf{r}_h$ is the two-dimensional (2D) relative coordinate, V_N an arbitrary 3D normalization volume for the phonon waves, λ denotes the exciton internal state, and the Fröhlich constant is[10]

$$C_F \equiv [2\pi e^2 \hbar\omega_{\mathrm{LO}} (\epsilon_{\infty}^{-1}-\epsilon_0^{-1})]^{1/2} , \tag{5}$$

with $\epsilon_0,\epsilon_{\infty}$ the low- and high-frequency dielectric constants. In Eq. (4) the polarization vector of the LO phonon has been taken in the $\mathbf{Q}+q\hat{\mathbf{z}}$ direction. The following points are significant in Eq. (4): (a) $\mathbf{Q}$ is fixed by momentum conservation but q is unrestricted; (b) only one particle in the exciton can change its confinement quantum number; (c) the internal exciton state can change only if $\mathbf{Q}\neq O$; (d) the exciton polarization and heavy- or light-hole character (i.e., all spins) are unchanged; (e) the process $\lambda'=\lambda$ with $\mathbf{Q}=0$ (the 2D analog of the "forbidden process" in 3D) is allowed in the 2D case providing either particle changes subband. In regard to (b) and (d), it should be noted that apparent violations of these selection rules can occur through hole-subband mixing to be discussed later.

The matrix elements of the photon-exciton interaction in the same approximation as Eq. (4) are

$$\langle X^{\mu} \mid -(e/m_0 c)\mathbf{A}\cdot\mathbf{p} \mid R^{\mu} \rangle = -C_A \lambda(0) \langle n_e \mid n_h \rangle \times \langle c \mid \hat{\boldsymbol{\mu}}\cdot\mathbf{p} \mid v \rangle L_N^{-1/2} , \tag{6}$$

$$C_A \equiv (2\pi\hbar e^2/\omega m_0^2 \epsilon_{\infty})^{1/2} ,$$

where $\lambda(\mathbf{r})$ is the normalized ($\int \mid \lambda \mid^2 d\mathbf{r}=1$) exciton internal wave function, $\mathbf{p}$ is the momentum operator, and L_N an arbitrary normalization length along $\hat{\mathbf{z}}$. This form is only useful for the so-called "allowed" transitions $n_e=n_h$ in the case of square wells, since it cannot account for the observed strength of the so-called "forbidden" transitions like E_{13h} or the DRRS reported here. The approximation in Eqs. (4) and (6) is the separation of the z and (x,y) motions of the hole based on neglecting the off-diagonal terms (subband mixing) (Refs. 17 and 18) in the valence-band effective-mass Hamiltonian H_h.

Subband mixing is discussed briefly in the Appendix for the case $\mathbf{K}=0$. If in the absence of mixing an exciton X is characterized by good quantum numbers v,n_h,λ (as well as c, n_e, and $\mathbf{K}=0$), and λ represents an optically active internal state of s symmetry (isotropic), then in the presence of mixing the optically active s-symmetry components of X have the same hole spin v. This is a consequence of the conservation of angular momentum (spin plus orbital) in subband mixing. We denote the Fourier transform of $\lambda(\mathbf{r})$ by $\lambda(\mathbf{k})$ such that $\lambda(\mathbf{r})=A_N^{-1/2}\sum_k \lambda(\mathbf{k})e^{i\mathbf{k}\cdot\mathbf{r}}$, where A_N is an arbitrary normalization area. The effect of mixing on the optical spectrum is described by the replacement

$$|n\rangle\lambda(k)\rightarrow\left(|n\rangle+\sum_{n'}{}'[C(k)]_{nn'}|n'\rangle\right)\lambda(k)\ ,$$
$$C(0)=0,\quad [C(k)]_{nn}=0\ , \tag{7}$$

where $[C(k)]_{nn'}$ gives the mixing. In lowest order in k, $[C(k)]_{nn'}=C_{nn'}k^2$ where $C_{nn'}$ is constant. We do not believe subband mixing need be considered in the scattering matrix element in Eq. (4), but it is essential in the optical matrix element Eq. (6).

The expansion of $C(k)$ in powers of k^2 can be obtained from perturbation theory (see the Appendix). For the case of interest here (the $13h$ transition), Eq. (6) is replaced by the leading term from subband mixing (second order in the term $\langle\frac{3}{2}|H_h|\frac{1}{2}\rangle$),

$$\langle X_{13h}^{\mu}|-(e/m_0c)\mathbf{A}\cdot\mathbf{p}|R^{\mu}\rangle = -C_A\langle c|\hat{\boldsymbol{\mu}}\cdot\mathbf{p}|v\rangle A_N^{-1/2}C_{3,1}\sum_k k^2\lambda(k)\ , \tag{8}$$

$$C_{3,1}=\frac{6}{5\pi^4}\frac{(m_h-m_l)^2}{m_l(9m_l-4m_h)}L_z^2\approx -0.017L_z^2\ ,$$

where L_z is the square-well width, m_h,m_l are the effective masses (units of m_0) for z motion, and the value is for GaAs quantum wells. To derive Eq. (8) it has been assumed that the confinement wave functions can be approximated by those for an infinite barrier. The Schrödinger equation for the exciton can be written approximately

$$\left(-\frac{\hbar^2}{2m_0m_r}\nabla^2-\frac{e^2}{\epsilon_0(r^2+\beta^2L_z^2)^{1/2}}\right)\lambda(r)=E_x\lambda(r)\ , \tag{9}$$

where m_r is the reduced effective mass, and the empirical constant β [representing an effective value for $(z_e-z_h)^2/L_z^2$] can be fixed by requiring, for example,

$$\langle 1e,1h|[a_B^2+(z_e-z_h)^2]^{-1/2}|1e,1h\rangle = (a_B^2+\beta^2L_z^2)^{-1/2}\ , \tag{10}$$

where $a_B=\epsilon_0\hbar^2/m_0m_re^2$ is the Bohr radius. Alternatively β can be fitted to known binding energies. The potential in Eq. (9) with $\beta=0.26$, when used in a variational calculation, gives binding energies in reasonable agreement as a function of L_z with more accurate variational treatments.[19] Regardless of the value of E_x, we have from Eq. (9) in the limit $r\rightarrow 0$,

$$A_N^{-1/2}\sum_k k^2\lambda(k)\approx(2/\beta a_BL_z)\lambda(0)\ , \tag{11}$$

so that Eq. (8) can be written in the form of Eq. (6) with the replacement

$$\langle 1e|3h\rangle\rightarrow(2C_{3,1}/\beta a_BL_z)\sim 0.12\ , \tag{12}$$

assuming $L_z=140$ Å, $a_B=160$ Å. The value of $\langle 1e|3h\rangle$ calculated in the conventional[7,20] way (no band mixing) is typically ~ 0.02–0.03. The value estimated in Eq. (12) is of sufficient size to account for the observed strength of E_{13h}.

The deformation potential interaction will not be discussed in detail. We mention here only that its nonvanishing matrix elements[21] are of the form $\langle\pm\frac{3}{2}|H_D|\mp\frac{1}{2}\rangle$ which couple heavy holes to light holes, as noted in Eq. (2), and thereby reverse the circular polarization of the emitted photon relative to that of the incident photon. Unlike H_F, H_D operates only on the holes.

The transition matrix element for the Fröhlich process of Eq. (1) is

$$T_F(\mu_s,\mu_i;q)=\frac{V_N^{-1/2}iC_RC_F\langle 3h|e^{-iqz}|1h\rangle|q|^{-1}}{L_N(\hbar\omega_i-E_{1h}-\hbar\omega_{\mathrm{LO}})(\hbar\omega_i-E_{13h})}\delta_{\mu s,\mu i}$$
$$C_R\equiv\frac{2\pi e^2\hbar|\lambda(0)|^2P_h|^2C_{3,1}}{(\omega_i\omega_s)^{1/2}m_0^2\epsilon_\infty\beta a_BL_z}\ , \tag{13}$$
$$P_h\equiv\langle\mp\tfrac{1}{2}|(p_x\pm ip_y)/\sqrt{2}|\mp\tfrac{3}{2}\rangle\ .$$

The lattice is here treated as a GaAs lattice. This process is diagonal in polarization indices μ_i,μ_s regardless of the basis chosen for expressing $\mu_i\mu_s$. The interaction with the lattice when dispersion of the phonon frequency is neglected can be regarded as the production of one phonon in the single effective mode (wave packet)

$$\mathbf{u}_F(z)=\hat{\mathbf{z}}\left(\sum_q|T_F(q)|^2\right)^{-1/2}V_N^{-1/2}\sum_q(q/|q|)e^{iqz}T_F(q)$$
$$=\hat{\mathbf{z}}A_N^{-1/2}(L_zI)^{-1/2}g_F(z)\ , \tag{14}$$

where

$$g_F(z)=\int_{-\infty}^{z}w_3(z)^*w_1(z)dz\ ,$$
$$I=L_z^{-1}\int_{-\infty}^{\infty}|g_F(z)|^2dz\ . \tag{15}$$

We have treated q as a continuous variable; for a superlattice q would be restricted to integer multiples of $2\pi/p$ (umklapp processes) where p is the period. In Eq. (14) $\mathbf{u}_F$ is the displacement of As relative to Ga atoms. Due to the orthogonality of the confinement wave functions $w_h(z)$, $g_F(z)$ vanishes outside the quantum well and the small penetration region in each barrier. This agrees with the fact that the phonon frequency observed (ω_{LO}) is that of GaAs. Assuming a square well and infinite barrier height, we obtain

$$g_F(z)=[\sin(4\pi z/L_z)+2\sin(2\pi z/L_z)](4\pi)^{-1}\ ,\quad |z|\le L_z/2\ , \tag{16}$$
$$g_F(0)=0,\quad |z|>L_z/2\ ,$$
$$I=(5/32\pi^2)\ .$$

For finite barriers Eq. (16) is still a reasonable representation if L_z is replaced with an effective width $L'_z > L_z$. A different single effective phonon mode is involved in the process of Eq. (2). Note that $\mathbf{u}_F$ is an even mode, $-\mathbf{u}_F(-z)=\mathbf{u}_F(z)$.

We believe the effective mode, which is a wave packet of bulk modes, is relevant to the experiments discussed here. However, the concept breaks down for very narrow wells ($L_z \sim 20$ Å) and for very large Al concentration in the barrier ($x \rightarrow 1$). Confined GaAs modes have been seen experimentally[2] and analyzed theoretically[22] for GaAs-AlAs superlattices. For narrow wells these are sufficiently split in frequency to be separately resolved; when that happens the superposition in Eq. (16) becomes meaningless.

From the transition rate ("Fermi's golden rule") $(2\pi/\hbar)\sum |T_{\rm if}|^2\delta(E_i-E_f)$, we obtain from Eq. (13) the scattering cross section (for the F process) per unit solid angle per unit area of quantum well (dimensionless)

$$A_N^{-1}\frac{d\sigma_s}{d\Omega}=\frac{4\pi\omega_s}{\omega_i}\left[\frac{\sigma_0}{a_B^2}\right]\left[\frac{L_z}{a_B}\right]\left[\frac{2C_{3,1}}{\beta a_B L_z}\right]^2\left[\frac{\epsilon_0}{\epsilon_\infty}-1\right][\lambda(0)a_B]^4 I\left[\frac{R_y|P_h^2/m_0|^2\hbar\omega_{\rm LO}}{|\hbar\omega_i-E_{1h}-\hbar\omega_{\rm LO}|^2|\hbar\omega_i-E_{13h}|^2}\right] \quad (17)$$

where $\sigma_0=(e^2/m_0c^2)^2$ and $R_y=e^2/2\epsilon_0 a_B$ is the Rydberg. Equation (17) includes the sum over q. From Eqs. (6) and (12) we obtain the absorption cross section per unit area of quantum well (dimensionless)

$$A_N^{-1}\sigma_a=\frac{4\pi^2}{n\alpha}\left[\frac{\sigma_0}{a_B^2}\right]\left[\frac{2C_{3,1}}{\beta a_B L_z}\right]^2[\lambda(0)a_B]^2\left[\frac{|P_h|^2}{m_0\hbar\omega_i}\right]\times[m_0c^2 f(\hbar\omega_i)]\,, \quad (18)$$

where $\alpha=e^2/\hbar c$, n is the refractive index, and $f(\hbar\omega_i)$ is a normalized line shape for the E_{13h} absorption, $\int f(E)dE=1$. We suppose that the absorption results in luminescence with a radiative efficiency η from heavy holes; the absence of light holes removes all emission polarized along $\hat{\mathbf{z}}$ that would be present in bulk material and adds this to the heavy-hole emission. It follows that Eq. (18) multiplied by $(\frac{3}{2})(\Delta\Omega/4\pi)\eta$ gives the emission into a detector of solid angle $\Delta\Omega$. Finally we can express the ratio of Raman scattered photons to luminescence photons entering the same detector

$$S\equiv\frac{\text{number of Raman photons}}{\text{number of luminescence photons}}=\frac{8n\alpha}{3\eta}\left[\frac{\epsilon_0}{\epsilon_\infty}-1\right]\left[\frac{L_z}{a_B}\right]\frac{[\lambda(0)a_B]^2 I}{m_0c^2 f(\hbar\omega_i)}\left[\frac{R_y(|P_h|^2/m_0)\hbar\omega_{\rm LO}\hbar\omega_s}{|\hbar\omega_i-E_{1h}-\hbar\omega_{\rm LO}|^2|\hbar\omega_i-E_{13h}|^2}\right]. \quad (19)$$

To treat the resonant case it is necessary to include damping $E_x \rightarrow E_x - i\Gamma_x$ in the exciton energies; we neglect the relatively small damping in the phonon $\hbar\omega_{\rm LO}$ which our DRRS experiment indicates (by the sharp linewidth) is about an order of magnitude smaller than that of the excitons. The damping can be due to exciton diffusion, recombination, relaxation to other subbands, or inhomogeneous broadening. We note that in general

$$f(\hbar\omega_i)|\hbar\omega_i-E_{13h}+i\Gamma_{13h}|^2=\Gamma_{13h}/\pi\,. \quad (20)$$

Based on the constants for GaAs (Refs. 19 and 23)

$$|P_h|^2/m_0=1.3\times10^4\ \text{meV},\quad R_y=3.7\ \text{meV},$$
$$\hbar\omega_{\rm LO}=36.7\ \text{meV},\quad a_B=160\ \text{Å}, \quad (21)$$
$$\epsilon_\infty=13.1,\quad \epsilon_0=11.1,\quad n=3.3\,,$$

and the parameters measured for the principle sample,

$$\hbar\omega_s=E_{1h}=1.534\times10^3\ \text{meV},$$
$$\Gamma_{1h}=2.1,\quad \Gamma_{13h}\approx2\ \text{meV}, \quad (22)$$
$$L_z=140\ \text{Å},\quad \eta=8.1\times1.0^{-3}\,,$$

and the rather reliable assumption $\lambda(0)a_B\sim\sqrt{(2/\pi)}$, we calculate

$$S\sim0.025(0.038)\,, \quad (23)$$

where the experimental value in parentheses is determined directly from Fig. 3(a). The agreement is highly satisfactory, and the calculated value being lower than the experimental value is in the right direction, and may indicate that the impurity-assisted FI process of Eq. (3) is making a contribution but not a dominant contribution. The small value $\eta S\sim2\times10^{-4}$ explains why only relatively dim samples are likely to exhibit DRRS in our apparatus.

The deformation potential process Eq. (2) is not important in the DRRS as evidenced by the polarization properties summarized in Table I. The F and D processes interfere[10] to produce the resultant transition matrix.

$$T(\mu_s,\mu_i;q)=T_F(\mu_s,\mu_i;q)+T_D(\mu_s,\mu_i;q)\,, \quad (24)$$

where T_F is given by Eq. (13) and T_D is similar except that: (a) $C_F|\mathbf{Q}+q\hat{\mathbf{z}}|^{-1}$ is replaced by a constant C_D containing the deformation potential, (b) the state $|1h\rangle$ is replaced by $|1l\rangle$, (c) the momentum matrix element enters

as $P_h P_l^*$ where $P_l = \pm P_h/\sqrt{3}$, (d) the energy E_{1h} is replaced by E_{1l}, (e) the circular polarization dependence is given by $[\mathrm{sgn}(\mu_i)\text{-}\mathrm{sgn}(\mu_s)]/2$ where $\mu = \pm 1$. Thus the D process contributes a negative circular polarization, which cannot be large because the observed circular polarization is very high and positive (+77%). It follows that for each q the polarization properties of T_D are given by

$$\begin{aligned} T_D(-,+) &= iT_D(x,y) = iT_D(x',x') \\ &= -T_D(+,-) = iT_D(y,x) \\ &= -iT_D(y',y') \\ T_D(x,x) &= T_D(y,y) = T_D(x',y') = T_D(y',x') \\ &= T_D(\pm,\pm) = 0 , \end{aligned} \tag{25}$$

where $(\pm)$ refer to $\hat{\boldsymbol{\mu}}_\pm = (\hat{\mathbf{x}} \pm i\hat{\mathbf{y}})/\sqrt{2}$ and $\hat{\mathbf{x}}', \hat{\mathbf{y}}'$ to $(\hat{\mathbf{x}}+\hat{\mathbf{y}})/\sqrt{2}$, $(\hat{\mathbf{x}}-\hat{\mathbf{y}})/\sqrt{2}$, respectively. T_F is proportional to the unit matrix referred to any of the bases (x,y), (x',y'), or $(+,-)$. As we have defined T_F, T_D [see Eq. (13) and (a)—(e) above] the quantities iT_F, iT_D are both real when ω_i, ω_s are far from the resonances of the energy denominators. In this case because of the factors "i" in Eq. (25) there would be no interference between them in any polarization configuration. However, if ω_s is in resonance with E_{1h} (the situation in DRRS observed here) the F scattering acquires a factor i due to the resonance and could interfere with the D scattering (for a given q) in the (x',x') and (y',y') configurations. However, the data of Table I (which correspond to the sum over q of $|T|^2$) indicate that the difference between these configurations is small (~ 0.04), which may mean that the D contribution is negligible; we return to this point later. We note that for a square well the effective mode for the D process is odd under reflection whereas that for the F process is even. This would suggest that the same phonon is not active in both processes, which would prevent interference.

Neither the F nor the D process contributes to the (y',x') configuration, yet this configuration has a very significant strength (0.27) in Table I. This indicates a significant effect due to spin relaxation. The relaxation of the electron and hole spins in the excitonic intermediate states produces a net effective polarization relaxation (PR) of the excitons accompanied by very small changes in energy. The width of the DRRS line (for varying ω_s with ω_i held fixed) is due to the width of the LO phonon plus the width of energy fluctuations from PR. This is to be distinguished from the width of the DRRS response (varying ω_i and ω_s with $\omega_i - \omega_s = \omega_{\mathrm{LO}}$) which is due to inhomogeneous broadening and damping [$\Gamma_{1h}, \Gamma_{13h}$ in Eq. (22)] of the exciton states. The distinction between PR and damping is that damping processes remove an exciton from the intermediate states which contribute to a scattering process such as shown in Eqs. (1), (2), or (3), whereas PR processes only reverse its circular polarization. We shall only discuss PR in a phenomenological way not attempting to describe its physical mechanisms in detail. Note, however, that the electron-hole exchange interaction alone does not couple different polarizations. The PR interaction H_{PR} couples the excitons X^μ to a reservoir (thermal bath) of states with continuous energy spectrum which we denote by an index ξ. In general the initial and final states ξ are not equal, but the integrated strength of the transition can be written as an average over just the initial ensemble of ξ using the general definition

$$\sum_{\xi\xi'} P_\xi |\langle \xi' | O | \xi \rangle|^2 \equiv \langle O^+ O \rangle_\xi , \tag{26}$$

where O is any operator on the reservoir and P_ξ is a probability distribution for the ξ ensemble. The T-matrix elements $T(\mu_s \mu_i; q, \mathbf{Q})$ in general are operators on the reservoir through inclusion of the interaction H_{PR} to all orders.

The quantities listed in Table I are integrated intensities for various polarization configurations which can be specified by a four-component vector $\mathbf{V}$ defined by its components V_γ as follows

$$\begin{aligned} &V_\gamma = \mu^*_{s\alpha} \mu_{i\beta}, \quad \gamma = \gamma(\alpha,\beta) , \\ &\gamma(+,+) = 1, \quad \gamma(+,-) = 2, \quad \gamma(-,+) = 3, \gamma(-,-) = 4 . \end{aligned} \tag{27}$$

Thus an arbitrary T matrix can be expanded in the form

$$T(\mu_s \mu_i; q, \mathbf{Q}) = \sum_\gamma V_\gamma T(\gamma; q, \mathbf{Q}) \tag{28}$$

in terms of the pure circular configurations γ. The vector $\mathbf{V}$ is given for each configuration in Table I. It is convenient to define a configuration density matrix

$$d_{\gamma\gamma'} = V_\gamma V^*_{\gamma'} \tag{29}$$

and write the integrated intensity (apart from an arbitrary factor) in the form

$$W\{\mathbf{V}\} = \mathrm{Tr}\{d\mathscr{R}\} , \tag{30}$$

where the Hermitian Raman matrix $\mathscr{R}$ is (apart from a factor)

$$\mathscr{R}_{\gamma\gamma'} = \sum_{q,Q} \langle T^\dagger(\gamma; q, \mathbf{Q}) T(\gamma'; q, \mathbf{Q}) \rangle_\xi . \tag{31}$$

The values in Table I are normalized to $\mathrm{Tr}\{\mathscr{R}\} = 2$, or $W\{1,0,0,0\} + W\{0,1,0,0\} = 1$.

The point-group symmetry of the GaAs(001) quantum-well Hamiltonian including an LO phonon along $\hat{\mathbf{z}}$ of wave vector $q, \mathbf{Q} = 0$ is C_{2v} which has reflection planes $x \to y$, $y \to x$ and $x \to -y$, $y \to -x$. From this it is easy to show that

$$\begin{aligned} &T(\pm,\pm;q,0) = T(\mp,\mp;q,0) , \\ &T(\pm,\mp;q,0) = -T(\mp,\pm;q,0) . \end{aligned} \tag{32}$$

Time-reversal symmetry also gives these relations. Because of the sum over $\mathbf{Q}$ in Eq. (31), $\mathscr{R}$, which may involve impurity assisted scattering, has the symmetry of the $\mathbf{Q} = \mathbf{O}$ case. It follows that $\mathscr{R}$ (denoted $\mathscr{R}^0$ for no PR) satisfies the symmetry relations

$$\mathscr{R}^0_{11}=\mathscr{R}^0_{44}=\mathscr{R}^0_{14}=\mathscr{R}^0_{41}\ \text{(no PR)}\ ,$$
$$\mathscr{R}^0_{22}=\mathscr{R}^0_{33}=-\mathscr{R}^0_{23}=-\mathscr{R}^0_{32}\ \text{(no PR)}\ , \tag{33}$$
$$\mathscr{R}^0_{12}=\mathscr{R}^0_{42}=-\mathscr{R}^0_{13}=-\mathscr{R}^0_{43}$$

for the pure Raman process without PR. Note that these relations do not assume anything about subband mixing. If the crystal is left with excitations of the PR reservoir, this symmetry will be reduced to

$$\mathscr{R}_{11}=\mathscr{R}_{44},\ \mathscr{R}_{22}=\mathscr{R}_{33}\ ,$$
$$\mathscr{R}_{14}=\mathscr{R}_{41},\ \mathscr{R}_{23}=\mathscr{R}_{32}\ \text{(with PR)}\ , \tag{34}$$
$$\mathscr{R}_{12}=\mathscr{R}_{42}=-\mathscr{R}_{13}=-\mathscr{R}_{43}\ ,$$

in which all relations connecting diagonal with off-diagonal components appearing in Eqs. (33) have been dropped. Using just the PR symmetry of Eqs. (34) and the components of **V** from Table I, we find the following general expressions for the integrated intensities (apart from a common factor) in the presence of PR

$$\begin{aligned}
&(+,+):\ \mathscr{R}_{11}\ ,\\
&(+,-):\ \mathscr{R}_{22}\ ,\\
&(x,x):\ \tfrac{1}{2}(\mathscr{R}_{11}+\mathscr{R}_{22}+\mathscr{R}_{14}+\mathscr{R}_{23})\ ,\\
&(y,x):\ \tfrac{1}{2}(\mathscr{R}_{11}+\mathscr{R}_{22}-\mathscr{R}_{14}-\mathscr{R}_{23})\ ,\\
&(x',x'):\ \tfrac{1}{2}[\mathscr{R}_{11}+\mathscr{R}_{22}+\mathscr{R}_{14}-\mathscr{R}_{23}-4\,\mathrm{Im}(\mathscr{R}_{12})]\ ,\\
&(y',y'):\ \tfrac{1}{2}[\mathscr{R}_{11}+\mathscr{R}_{22}+\mathscr{R}_{14}-\mathscr{R}_{23}+4\,\mathrm{IM}(\mathscr{R}_{12})]\ ,\\
&(y',x'):\ \tfrac{1}{2}(\mathscr{R}_{11}+\mathscr{R}_{22}-\mathscr{R}_{14}+\mathscr{R}_{23})\ .
\end{aligned} \tag{35}$$

Note that symmetry ensures that $(x,y)=(y,x)$, $(x',y')=(y',x')$, and $(x,x)=(y,y)$. These relations, Eqs. (34) and (35), are valid for any combination of mechanisms, since no assumption has been made about the reflection symmetry, if any, of the phonon, which would come in through the sum over q in Eq. (31).

The consistency of the data can be checked against the two relations

$$\underset{(1.02\pm0.04)}{(x,x)}+\underset{(1.00)}{(y,x)}=(+,+)+(+,-)=(y',x')+\underset{(1.06\pm0.05)}{\tfrac{1}{2}[(x',x')+(y',y')]}\ . \tag{36}$$

We have indicated below each quantity its value from Table I. One of these relations can also be written

$$\underset{(-0.04\pm0.06)}{(y,x)}-(y',x')=\tfrac{1}{2}[(x',x')+(y',y')]-\underset{(0\pm0.03)}{(x,x)}=-\mathscr{R}_{23}\ , \tag{37}$$

which is of interest because the right-hand side equals $-\mathscr{R}_{23}$ which can only come from the D process Eq. (2). Thus the data do not indicate any significant D process in the DRRS, since the presence of substantial linear and circular polarization shows that the vanishing of $\mathscr{R}_{23}$ cannot be attributed to PR. However, it is of interest to examine.

$$(x',x')-(y',y')=-4\,\mathrm{Im}(\mathscr{R}_{12})=-0.07\pm0.05\ . \tag{38}$$

where the value comes from Table I. This is the interference between the F and D processes (after reduction by PR) studied for bulk GaAs by Menéndez and Cardona.[10] As previously mentioned, the F and D processes are expected to have a quadrature phase relationship near the DRRS peak so that $\mathrm{Im}(\mathscr{R}_{12})$ is nonvanishing if the D process is significant, unless different reflection ($z\rightarrow -z$) symmetries cause the sum over q $\sum_q$ to vanish in Eq. (31) for the interference term.

To analyze Eq. (38) further, and to discuss PR in DRRS in a quantitative way, it is necessary to parametrize the PR. We write $\mathscr{R}$ in the form (satisfying $\mathscr{R}_{11}+\mathscr{R}_{22}=1$)

$$\mathscr{R}_{\gamma\gamma'}=\frac{\mathscr{R}^0_{\gamma\gamma'}+\frac{1}{2}(\tau_0/\tau_1)\delta_{\gamma\gamma'}}{1+(\tau_0/\tau_1)\delta_{\gamma\gamma'}+(\tau_0/\tau_2)(1-\delta_{\gamma\gamma'})}\ , \tag{39}$$

where the times τ_0,τ_1,τ_2 are intended to characterize the exciton lifetime, the diagonal relaxation of $\mathscr{R}$, and the off-diagonal relaxation (dephasing) of $\mathscr{R}$, respectively. We present Eq. (39) without derivation as reasonable in the absence of a detailed theory of PR for DRRS comparable with the formal theory for polarized photoluminescence[24] and optical dephasing.[25] We believe that the presence of sizable PR in DRRS is closely associated with the well-known connection[26] between resonance Raman scattering and the sequential process of absorption followed by luminescence to which Eq. (39) would directly apply. The process (y',x'), which depends entirely on PR, gives us the result

$$\begin{aligned}
&(y',x')=\tfrac{1}{2}(\tau_0/\tau_2)/(1+\tau_0/\tau_2)=0.27\pm0.04\ ,\\
&\tau_0/\tau_2=1.2\pm0.5\ .
\end{aligned} \tag{40}$$

If $\mathscr{R}^0_{22}/\mathscr{R}^0_{11}\ll 1$ is neglected (corresponding to negligible D process), the circular polarization gives

$$\begin{aligned}
&\rho=(1+\tau_0/\tau_1)^{-1}=0.77\pm0.01\ ,\\
&\tau_0/\tau_1=0.30\pm0.02\ .
\end{aligned} \tag{41}$$

From Eq. (38) the interference term before PR is

$$\mathrm{Im}(\mathscr{R}^0_{12})=(1+\tau_0/\tau_2)\mathrm{Im}(\mathscr{R}_{12})=-0.04\pm0.04\ . \tag{42}$$

This is consistent with the vanishing of the interference of the F and D processes due to opposite parity of the phonons involved when the well has a symmetry plane. However, with a small asymmetry of the well, interference becomes allowed and could be a more sensitive indicator of

the presence of D scattering than $\mathscr{R}_{23}$ in Eq. (37). Therefore it is worth noting that through the rigorous inequality

$$|\,\mathrm{Im}(\mathscr{R}^0_{12})\,| < (\mathscr{R}^0_{22}\mathscr{R}^0_{11})^{1/2}$$

it follows that a lower limit on the D scattering relative to the F scattering is given by

$$\mathscr{R}^0_{22}/\mathscr{R}^0_{11} > |\,\mathrm{Im}(\mathscr{R}^0_{12})\,|^2 \sim 0.0025(1\pm 1)\ , \tag{43}$$

where the mean and rms deviation are obtained by assuming a Gaussian distribution in Eq. (42). This is consistent with the D process being negligible as noted above.

The processes associated with τ_0 and τ_1 do not contribute to the width Γ of the DRRS peak which depends only on the LO-phonon broadening, which we interpret as an equivalent lifetime τ_{LO}, and the dephasing time τ_2. If the broadening is Lorentzian, we have

$$2\Gamma/\hbar = \tau_{\mathrm{LO}}^{-1} + \tau_2^{-1}\ . \tag{44}$$

Experimentally the true half-width Γ was not accurately determined because the DRRS line had only slightly greater width (FWHM ≈ 0.38 meV) than the exciting laser line (FWHM ≈ 0.33 meV). Assuming for convenience Gaussian broadening for both lines gives the estimate $\Gamma \lesssim 0.1$ meV which should be regarded as an upper limit for Γ. This is about what we would expect[27] for the LO phonon, from which we conclude that most probably

$$\begin{aligned} &\tau_2 \gg 3\times 10^{-12}\ \mathrm{s}\ , \\ &\tau_{\mathrm{LO}} \sim 3\times 10^{-12}\ \mathrm{s}\ . \end{aligned} \tag{45}$$

It now follows from Eq. (40) that τ_0 is much too long to explain the resonance width (FWHM ≈ 4 meV) of the DRRS which we attribute to inhomogeneous broadening rather than exciton diffusion or recombination.

We believe that τ_{LO} cannot be attributed to effects due to the combination of large q and phonon dispersion, which in the case of superlattices would be called umklapp broadening.[4] According to Eq. (13) the distribution in q of the phonons is proportional to the quantity $|\langle 3h\,|\,e^{-iqz}\,|\,1h\rangle/q\,|^2$ which has a peak at $qL_z/2\pi \sim 1.1$ and a width (FWHM) $\Delta qL_z/2\pi \sim 1.2$. It then follows from the known dispersion[28] of ω_{LO} in GaAs that the spread (FWHM) in phonon energies is $\hbar\Delta\omega_{\mathrm{LO}} \sim 0.026$ meV which is about 8 times smaller than the observed value (0.2 meV). The concept of an effective phonon mode is valid in this case because the decay time for the wave packet is about 8 times longer than the phonon lifetime.

We have not been able to determine the separate contributions of the F process Eq. (1) and the FI process Eq. (3), since both have the same symmetry properties, and interference of the F process with the D process Eq. (2) is negligible. A consideration of the magnitude of the scattering compared with normal luminescence in Eq. (23) led to the conclusion that there may be significant FI scattering of comparable strength to the F scattering. We now speculate that the rather large PR present in the DRRS is due entirely to FI processes. It is reasonable that these processes involving $\mathbf{Q}\neq\mathbf{0}$ phonons and $\mathbf{K}\neq\mathbf{0}$ excitons are more subject to spin-flipping interactions than are the $\mathbf{Q}=\mathbf{0}$, $\mathbf{K}=\mathbf{0}$ processes of the F process. Therefore we suppose

$$\begin{aligned} &\mathscr{R} = f\mathscr{R}^F + (1-f)\mathscr{R}^{FI}\ , \\ &\mathscr{R}^F = \mathscr{R}^{0,F} = \mathscr{R}^{0,FI} = \mathscr{R}^0\ , \\ &\tau_2^{FI} = 0,\quad \tau_0^F = \tau_0^{FI} = \tau_0\ , \end{aligned} \tag{46}$$

where f is the fraction of F processes, and we seek to determine f, τ_1^{FI} from the effective values of τ_1, τ_2 fitted to experiment. The solution is

$$\begin{aligned} &f = (1+\tau_0/\tau_2)^{-1}\ , \\ &\frac{\tau_0}{\tau_1^{FI}} = \frac{(1+\tau_0/\tau_2)(\tau_0/\tau_1)}{(\tau_0/\tau_2)-(\tau_0/\tau_1)}\ . \end{aligned} \tag{47}$$

From the values in Eqs. (40) and (41) we obtain,

$$f \sim 0.45,\quad \tau_0/\tau_1^{FI} \sim 0.73\ , \tag{48}$$

which would indicate 55% of the scattering may be impurity assisted.

The higher-order processes involving 2,3,4 LO phonons detected in these experiments seem to require the resonance $E_{13h} - E_{1h} = \hbar\omega_{\mathrm{LO}}$ to be observable. For the 2 LO process we suggest the mechanism

$$\mathscr{R}_i - - \xrightarrow{\mathbf{A}\cdot\mathbf{p}} (X_{3h}) \xrightarrow{F} (X'_{13h}+L') \xrightarrow{F} (X_{1h}+L'+L'') \xrightarrow{\mathbf{A}\cdot\mathbf{p}} \mathscr{R}_s + L' + L'' \tag{49}$$

in the notation of Eq. (1). The assignment of the nonresonant virtual state to X_{3h} is speculative; actually a large number of other virtual states may also contribute significantly. The higher-order processes 3 LO and 4 LO have additional nonresonant virtual states which we cannot identify following the initial photon state R_i, but otherwise finish like Eq. (49). All these transitions, therefore, have matrix elements with two resonant denominators and may appropriately be called DRRS.

In treating the exciton-phonon interaction we have neglected subband mixing. This leads to definite parity for the phonon (opposite for F and D processes) in the case of symmetric wells. The question arises whether inclusion of subband mixing could destroy the parity of hole confinement states and hence the parity of the phonon. It is known[29] that the exciton transition E_{12h}, which would seem to be parity forbidden, is sometimes observed in excitation spectra and can be explained by calculations which include subband mixing. The explanation is that photon absorption is not to the $1s$ ground state of X_{12h} but to the $2p$ excited state (X^*_{12h}) through its coupling (subband mixing) to the $1s$ ground state of X_{1l}; subsequently X^*_{12h} thermalizes to X_{1h} from which luminescence is observed with positive circular polarization (heavy-hole-like), since the electron spin does not have time to thermalize. It is clear that in DRRS angular momentum (which starts and ends at zero) would require an even number of couplings for a nonvanishing matrix element, whereas reversing the parity of the phonon would require an odd number; thus subband mixing can not destroy the parity (if any) of the phonon.

IV. SUMMARY

Doubly resonant LO-phonon Raman scattering (DRRS) has been observed in many special GaAs-$Ga_{1-x}Al_xAs$ quantum-well structures as a very sharp (FWHM ~ 0.4 meV) component in the E_{1h} ground-state-exciton luminescence under excitation at photon energies $E_{1h}+n\hbar\omega_{LO}$ ($n=1,2,3,4$). In most of the special samples, having many square wells or in one case a single square well, the "forbidden" exciton E_{13h} was resonant with the first-order Raman scattering $E_{13h}=E_{1h}+\hbar\omega_{LO}$. In several other square-well samples the resonance involved $E_{1l}=E_{2h}-\hbar\omega_{LO}$. For one sample having half-parabolic wells the resonance was with $E_{21h}=E_{1h}+\hbar\omega_{LO}$. The DRRS peak is much less sensitive to temperature and incident intensity than the ordinary luminescence. Detailed polarization studies on the first order DRRS at 6 K were carried out for one sample, the principle sample, giving the integrated intensities listed in Table I for various configurations. The circular polarization (77%) was nearly 3 times that of the broad luminescence peak, and high optical alignment (linear polarization) was observed ($\sim 50\%$) which is ordinarily not observed in quantum-well luminescence. A brief report on this work has appeared elsewhere.[30]

The theoretical discussion of the principal sample aims to establish the mechanism of the one-phonon DRRS, to account quantitatively for its strength, and to interpret the observed polarization properties. The important mechanism is found to be the Fröhlich interaction which produces the LO phonon and scatters an exciton from the $1h$ subband to the $1h$ subband, possibly assisted by impurity scattering. To account for the strength of DRRS it was necessary to derive by perturbation theory the effect of subband mixing in the exciton wave function. It was shown for the Fröhlich process that the calculated ratio (~ 0.025) of Raman scattered photons to ordinary luminescence photons entering a detector is in satisfactory agreement with the experimental value (~ 0.038). However, there could also be a contribution from the impurity-assisted Fröhlich process of comparable magnitude. An explicit expression is obtained for the effective LO mode involved in the Fröhlich process on the assumption of a uniform GaAs lattice. This mode is shown to be completely confined to the quantum well, so no error is introduced by the uniform GaAs model. The conditions for the validity of an effective mode are discussed. The deformation potential interaction has also been described and the data carefully examined for evidence of scattering by this mechanism, in particular, interference between it and the Fröhlich mechanism. It is noted that interference is forbidden by symmetry for symmetric wells. Unequivocal conclusions were reached that the deformation potential contribution is negligible in the DRRS observed here. The data clearly showed the presence of hole and electron spin relaxation resulting in a polarization relaxation in the DRRS. In order to analyze the data it was necessary to determine the implications of symmetry with and without relaxation. It was shown that the data are consistent with the expected symmetry of the Raman matrix. The effects of relaxation evidenced in the data are interpreted in terms of two parameters τ_1/τ_0 and τ_2/τ_0, where τ_0 is the exciton lifetime in the states relevant for DRRS, τ_1 is the decay time for circular polarization, and τ_2 is the dephasing time (coherence decay time) between states of definite circular polarization. It was not possible to obtain values for τ_0,τ_1,τ_2, but it was concluded that the resonance response of the DRRS is inhomogeneously broadened, and the linewidth is that of the LO phonon. The contribution of the impurity-assisted Fröhlich process was estimated to be $\sim 55\%$ on the assumption that all relaxation is due to this process. The higher-order ($n=2,3,4$) Raman transitions observed are attributed to the Fröhlich mechanism acting through a series of $n+1$ virtual excitons with the last two being the $1h$ and $1h$ involved in the $n=1$ process.

ACKNOWLEDGMENTS

We wish to thank S. K. Sputz for assistance in obtaining the data, and W. Wiegmann and J. H. English for assistance in growing the MBE structures, and A. Pinczuk for helpful discussions.

APPENDIX

Consider an exciton at rest ($\mathbf{K}=0$); the hole wave vector can then be taken to be $\mathbf{k}$, the wave vector conjugate to the relative coordinate $\mathbf{r}$ in the (x,y) plane. Except for an arbitrary and unimportant phase factor the subband mixing term in the hole Hamiltonian H_h is[31]

$$\langle \tfrac{3}{2} \mid H_h \mid \tfrac{1}{2} \rangle = (3^{1/2}/4)(m_{lh}^{-1}-m_{hh}^{-1}) \times (1+a)^{1/2}\hbar^{-2}(-k_x+ik_y)(-i\nabla_z) , \quad \text{(A1)}$$

where $\nabla_z=\partial/\partial z_h$, a is an anisotropy parameter which for convenience we take to be zero (spherical model), and m_{lh} and m_{hh} are the light- and heavy-hole masses for z motion. Different subbands are coupled by ∇_z while at the same time the angular momentum is lowered by the operator $(-k_x+ik_y)$ so as to conserve total (spin plus orbital) angular momentum. The wave function in $\mathbf{k}$ space can be written $\lambda(\mathbf{k}) \mid n,v \rangle$, where v denotes spin and n is a confinement quantum number. We have indicated in Eq. (7) an expansion in which states n' are mixed with state n with v and k unchanged. The leading term in $[C(k)]_{nn'}$ is

$$[C(k)]_{nn'}=\sum_{n'',v''}{}' \frac{\langle n',v \mid H_h \mid n'',v'' \rangle \langle n'',v'' \mid H_h \mid n,v \rangle}{(E_{nv}-E_{n'v})(E_{nv}-E_{n''v''})} , \quad \text{(A2)}$$

where $n''\neq n$, $n''\neq n'$, and

$$E_{nv}=W_{nv}+\hbar^2k^2/2m_{vt} , \quad \text{(A3)}$$

where W_{nv} is the confinement energy and m_{vt} is the transverse mass for spin v. We write W_{nv} for a square well in the approximation of infinite barrier height and neglect the transverse kinetic energy in Eq. (A3). Only one intermediate state $\mid 2,\tfrac{1}{2} \rangle$ contributes to Eq. (A2) in the case of interest here $n=3$, $n'=1$, $v=\tfrac{3}{2}$. Thus the relevant energies in Eq. (A2) are

$$E_{3,3/2}=(\hbar^2/2m_{hh})(3\pi/L_z)^2 ,$$
$$E_{2,1/2}=(\hbar^2/2m_{lh})(2\pi/L_z)^2 , \quad \text{(A4)}$$
$$E_{1,3/2}=(\hbar^2/2m_{hh})(\pi/L_z)^2 ,$$

and the matrix elements of ∇_z are

$$\langle 2 \mid \nabla_z \mid 3 \rangle = 24/5L_z ,$$
$$\langle 1 \mid \nabla_z \mid 2 \rangle = -8/3L_z . \quad \text{(A5)}$$

Now substitution into Eq. (A2) leads to $C_{3,1}k^2$ with $C_{3,1}$ given by Eq. (8).

[1]J. E. Zucker, A. Pinczuk, D. S. Chemla, A. C. Gossard, and W. Wiegmann, Phys. Rev. Lett. **51**, 1293 (1983); **53**, 1280 (1984).
[2]A. K. Sood, J. Menéndez, M. Cardona, and K. Ploog, Phys. Rev. B **32**, 1412 (1985).
[3]P. Manuel, G. A. Sai-Halasz, L. L. Chang, Chin-An Chang, and L. Esaki, Phys. Rev. Lett. **37**, 1701 (1976).
[4]G. A. Sai-Halasz, A. Pinczuk, P. Y. Yu, and L. Esaki, Solid State Commun. **25**, 381 (1978).
[5]R. C. Miller, D. A. Kleinman, O. Munteanu, and W. T. Tsang, Appl. Phys. Lett. **39**, 1 (1981).
[6]R. C. Miller, D. A. Kleinman, W. A. Nordland, Jr., and A. C. Gossard, Phys. Rev. B **22**, 863 (1980).
[7]R. C. Miller, D. A. Kleinman, and A. C. Gossard, Phys. Rev. B **29**, 7085 (1984).
[8]A. Mooradian and G. B. Wright, Solid State Commun. **4**, 431 (1966).
[9]J. L. Merz, A. S. Barker, Jr., and A. C. Gossard, Appl. Phys. Lett. **31**, 117 (1977).
[10]J. Menéndez and M. Cardona, Phys. Rev. B **31**, 3696 (1985).
[11]R. C. Miller, A. C. Gossard, and D. A. Kleinman, Phys. Rev. B **32**, 5443 (1985).
[12]R. M. Martin, Phys. Rev. B **4**, 3676 (1971).
[13]R. Zeyher, C-S. Ting, and J. L. Birman, Phys. Rev. B **10**, 1725 (1974).
[14]R. Merlin, C. Colvard, M. Klein, H. Morkoc, A. Cho, and A. C. Gossard, Appl. Phys. Lett. **36**, 43 (1980).
[15]C. Weisbuch, R. C. Miller, R. Dingle, A. C. Gossard, and W. Wiegmann, Solid State Commun. **37**, 219 (1981).
[16]R. C. Miller and D. A. Kleinman, J. Lumin. **30**, 520 (1985).
[17]Y.-C. Chang and J. N. Schulman, Appl. Phys. Lett. **43**, 536 (1983).
[18]G. D. Sanders and Y-C. Chang, Phys. Rev. B **32**, 5517 (1985).
[19]R. C. Miller, D. A. Kleinman, W. T. Tsang, and A. C. Gossard, Phys. Rev. B **24**, 1134 (1981).
[20]R. Dingle, Festkorperprobleme **15**, 21 (1975).
[21]G. L. Bir and G. E. Pikus, *Symmetry and Strain-induced Effects in Semiconductors* (Wiley, New York, 1974), Eq. (32.54).
[22]S.-K. Yip and Y.-C. Chang, Phys Rev. B **30**, 7037 (1984).
[23]P. Lawaetz, Phys. Rev. B **4**, 3460 (1971).
[24]G. Fishman, C. Hermann, and G. Lampel, J. Phys. C **35**, 3 (1974).
[25]K. E. Jones and A. H. Zewail, in *Advances in Laser Chemistry,* edited by A. H. Zewail (Springer, Berlin, 1978), p. 196.
[26]M. V. Klein, Phys. Rev. B **8**, 919 (1973).
[27]A. Klyuchikhin, S. Permogorov, and A. Reznitskii, Zh. Eksp. Teor. Fiz. **71**, 2230 (1976) [Sov. Phys.—JETP **44**, 1176 (1976)].
[28]J. L. T. Waugh and G. Dolling, Phys. Rev. **132**, 2410 (1963).
[29]R. C. Miller, A. C. Gossard, G. D. Sanders, Y.-C. Chang, and J. N. Schulman, Phys. Rev. B **32**, 8452 (1985).
[30]R. C. Miller, D. A. Kleinman, and A. C. Gossard, Solid State Commun. **60**, 213 (1986).
[31]J. M. Luttinger and W. Kohn, Phys. Rev. **97**, 869 (1955).